Selective Turn-On Ammonia Sensing Enabled by High-Temperature Fluorescence in Metal−Organic Frameworks with Open Metal Sites

Natalia B. Shustova,[†] Anthony F. Cozzolino,[†] Sebastian Reineke,[‡] Marc Baldo,[‡] and Mircea Dincă*,[†]

[†]Department of Chemistry and [‡]Department of Electrical Engineering and Computer Science, Massachusetts Institute of Technology, Cambridge, Massachusetts 02139, United States

S *Supporting Information*

ABSTRACT: We show that fluorescent molecules incorporated as ligands in rigid, porous metal−organic frameworks (MOFs) maintain their fluorescence response to a much higher temperature than in molecular crystals. The remarkable high-temperature ligand-based fluorescence, demonstrated here with tetraphenylethylene- and dihydroxyterephthalate-based linkers, is essential for enabling selective and rapid detection of analytes in the gas phase. Both $Zn_2(TCPE)$ (TCPE = tetrakis(4-carboxyphenyl)ethylene) and $Mg(H_2DHBDC)$ (H_2DHBDC^{2-} = 2,5-dihydroxybenzene-1,4-dicarboxylate) function as selective sensors for ammonia at 100 °C, although neither shows NH_3 selectivity at room temperature. Variable-temperature diffuse-reflectance infrared spectroscopy, fluorescence spectroscopy, and X-ray crystallography are coupled with density-functional calculations to interrogate the temperature-dependent guest−framework interactions and the preferential analyte binding in each material. These results describe a heretofore unrecognized, yet potentially general property of many rigid, fluorescent MOFs and portend new applications for these materials in selective sensors, with selectivity profiles that can be tuned as a function of temperature.

One of the premier performance metrics in chemical sensing applications is chemical selectivity, the ability to detect a given molecular species while avoiding false positives from other potential interferents. When high selectivity is coupled with low detection limits and with signal transduction mechanisms that allow for facile device implementation, chemical sensing enables a range of applications in the defense, food packaging, and environmental monitoring sectors, among others. Microporous MOFs are attractive for this purpose because, in principle, they can be tuned to detect only specific analytes,[1] thus offering good selectivity, and they can exhibit a high density of analyte adsorption/binding sites, thereby enabling lower detection limits. Although various signal transduction mechanisms have been probed in MOFs, those based on changes in luminescence are favored thus far, partly because fluorescence detection obviates the necessity for film fabrication or other processing, a significant challenge with these materials.[2,3] Despite the potential advantages, fluorescent MOF sensors[4−9] typically operate by luminescence quenching,[10−14] a "turn-off" mechanism that is seldom specific and is

generally more difficult to detect. A much more attractive mechanism involves fluorescence "turn-on", where interaction of the MOF with an analyte either turns a "dark" material into a luminescent one or causes a shift from the initial maximum wavelength of the emission peak, λ_i, to a final value, λ_f. Monitoring the luminescence response at this single wavelength λ_f is read as an increase in the luminescence intensity (Figure 1). MOFs that display luminescence turn-on upon contact with
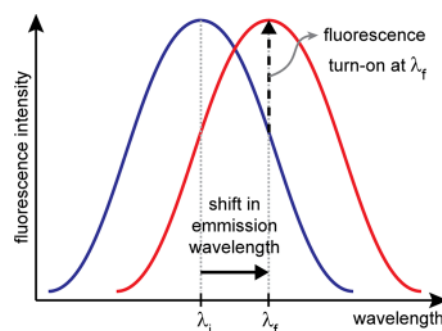

Figure 1. Illustration of the fluorescence shift, turn-on mechanism of chemical sensing, where detection monitoring at λ_f will reveal an intensity increase upon interaction with an analyte.

analytes are rare;[6] those that exhibit both turn-on fluorescence *and* selectivity for a single chemical species are rarer still.[15,16]

Here, we demonstrate that fluorescent MOFs maintain their luminescence up to high temperatures, in contrast to molecular crystals or polymers, which often lose their fluorescence near their melting or glass transition temperature.[17,18] Notably, the high-temperature fluorescence exhibited by the two materials studied here enables the selective detection of gaseous ammonia at 100 °C. Interaction of NH_3 with $Zn_2(TCPE)$ (**1**) and $Mg(H_2DHBDC)$ (**2**) causes fluorescence shifts and turn-on luminescence responses preferentially over a variety of potential interferents such as water, methanol, larger amines, and other gases. The NH_3 sensing response can be reversed in **2** upon short evacuation without additional heating, suggesting potential applications in reversible NH_3 sensors.[19]

Fluorescent organic crystals and polymers typically become non-emitting upon melting or glassifying, such that their use in luminescence-based devices can be limited even at moderately high temperatures.[17,18] We showed recently that one means to

modulate the luminescence response of small molecules, such as tetraphenylethylene (TPE), is to incorporate them within rigid MOFs such as **1** (Figure S1),[20,21] where vibrational modes responsible for fluorescence quenching are minimized.[22] Here, we show that these vibrational modes are suppressed even at higher temperatures and that **1** maintains its fluorescence up to at least 350 °C, close to its decomposition temperature of 400 °C, as determined by thermogravimetric analysis (TGA, Figure S2). To investigate the temperature-dependent luminescence of **1**, we collected emission spectra of a powdered sample as it was gradually heated in air inside of a reaction chamber (see Supporting Information for additional details).[23] The fluorescence intensity, I, at each temperature point was divided by the intensity observed at room temperature, I_0, and is plotted as I/I_0 vs temperature in Figure 2, which also displays data for a
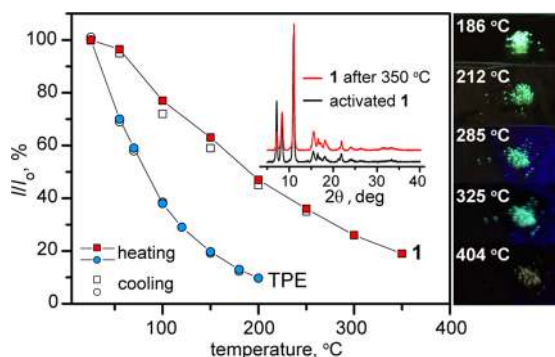

Figure 2. Temperature-dependent fluorescence decay profiles of **1** (squares) and TPE (circles), where I_0 is the fluorescence intensity at room temperature. Heating and cooling cycles are represented as filled and open symbols, respectively. The inset shows PXRD patterns of activated **1** and after heating at 350 °C in air. The optical micrographs show fluorescent **1** (λ_{ex} = 350 nm) upon heating at various temperatures in air.

cooling cycle. As shown in the figure, **1** loses 50% of its initial fluorescence intensity only at $T_{1/2}$ = 190 °C. Furthermore, **1** does not lose its crystallinity or luminescence response upon cooling and repeating the cycle at least three times. This is in stark contrast with TPE itself, also shown in Figure 2, which under identical experimental conditions dramatically loses its fluorescence ($T_{1/2}$ = 83 °C). In fact, TPE becomes virtually non-fluorescent near its melting point of 224 °C, when presumably its low-energy vibrational modes responsible for fluorescence quenching are reactivated.[24] Thus, TPE-borne luminescence persists to a much higher temperature when TPE is inserted in a rigid MOF. At 200 °C, for instance, I/I_0 for **1** was 47%, approximately 5 times larger than that of TPE, which was only 10%.

We surmised that the temperature-persistent luminescence of **1** could be used to modulate its response toward various gas-phase analytes. Thus, exposure of activated **1** to ammonia, triethylamine, ethylenediamine (en), *N,N*-diethylformamide (DEF), and water vapors at room temperature shifted its emission maximum by 0–23 nm. However, as shown in Figure 3, monitoring the effect of these analytes at 100 °C showed that only ammonia exposure led to a significant shift of the emission maximum from 487 to 511 nm, thus revealing a remarkable selectivity for NH_3 detection. Unfortunately, ammonia binding also caused an irreversible phase change in **1** to an unidentified crystalline form (Figure S3), which suggested that this material would not be effective in a reversible sensing application.
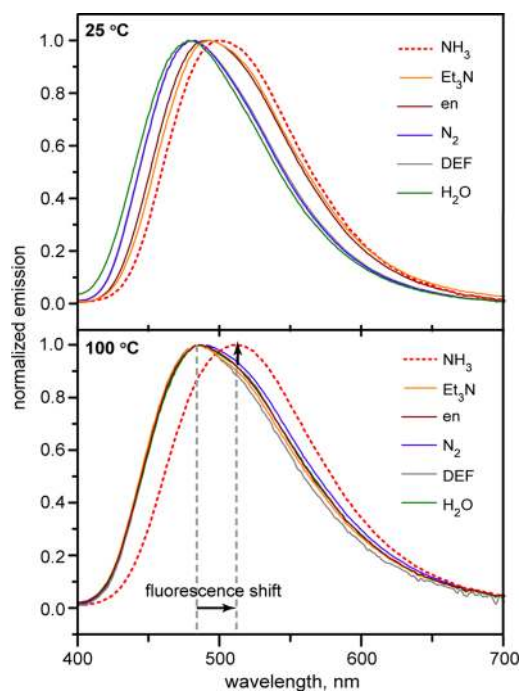

Figure 3. In situ normalized emission spectra (λ_{ex} = 350 nm) of **1** exposed to various analytes at room temperature and 100 °C.

However, we were interested in the mechanism leading to the preferential sensing. We reasoned that the selectivity may be due to the differential strength of analyte binding to the Zn^{2+} ions in the $Zn_2(O_2C-)_4$ secondary building units of **1**. To test this hypothesis, we calculated the binding energies of NH_3 and H_2O to the paddlewheel unit using density functional theory (DFT) and found that NH_3 binding was more favorable than H_2O binding by 38 kJ/mol (Table S1 and Figure S4). This finding suggested that, although both NH_3 and H_2O may affect the electronic structure of the $TCPE^{4-}$ by binding to Zn^{2+} in **1**, only the former does so effectively at 100 °C. More importantly, these results also implied that the selectivity may be observed in other thermally stable, fluorescent MOFs with open metal sites and that a reversible NH_3 sensor may be found among reported materials that fit these criteria.

One material candidate was $Mg(H_2DHBDC)$ (**2**), wherein Mg^{2+} ions coordinated by four H_2DHBDC^{2-} units and two *N,N*-dimethylformamide (DMF) molecules form $Mg(O_2C-)$ chains (Figures S4 and S5).[25] Compound **2** is thermally stable up to 250 °C (Figure S6), and was reported to retain its structure after desolvation at 220 °C.[25] Our attempts to activate **2** in the 170–220 °C temperature range caused a structural change, however, as evidenced by the powder X-ray diffraction (PXRD) patterns in Figures 4 and S7. To identify the structure of desolvated **2** (**2d**), we first performed variable-temperature infrared (VT-IR) spectroscopy and determined that the stretches associated with bound DMF molecules are gradually lost upon heating as-synthesized **2** at 120 °C for 12 h (Figure S6). Accordingly, we undertook a variable-temperature single-crystal X-ray diffraction study and slowly heated a crystal of as-synthesized **2** to 393 K while monitoring its unit cell parameters. As shown in Tables S2 and S3, no structural transformations occurred while ramping from 100 to 393 K. However, prolonged heating at 393 K for 12 h led to significant changes in the unit cell parameters, presumably brought by the loss of DMF molecules in **2d**, in accordance with the IR data.
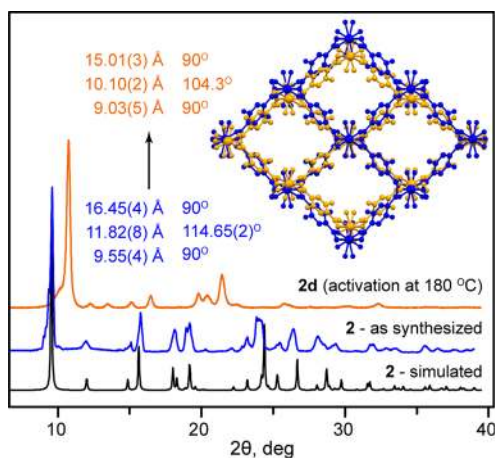
Figure 4. PXRD patterns of **2** and **2d**. The inset shows overlaid structures of **2** (blue) and modeled for **2d** (orange). The unit cell parameters for **2** (blue) and **2d** (orange) were determined by single-crystal X-ray diffraction studies.

Although damage to the crystal during this treatment prevented the collection of a full data set, we used the new unit cell parameters to model the structure of **2d** using an original Matlab routine that we reported recently (Figure S8).[26] As shown in Figures 4 and S7, the changes evidenced in the PXRD patterns are caused by a relatively small breathing mode that occurs upon desolvation but does not disrupt the original bonding of as-synthesized **2**.

Having ascertained that the connectivity of **2** remains intact upon desolvation, we tested the response of **2d** to various gas-phase analytes at temperatures up to 100 °C. We were intrigued to discover that **2d** had been reported as a selective CO_2 adsorbent.[25] Accordingly, we investigated its fluorescence response upon exposure to CO_2 but found no changes in its emission profile at −78, 25, or 100 °C (Figures S9−S11). In contrast, exposure of **2d** to NH_3 gas at 100 °C for less than 1 min caused a significant shift in its emission maximum (Figures 5 and S12−S14). No changes were observed upon exposure to methanol or water vapors at this temperature even after 2 h (Figures 5 and S15, S16). The lack of changes in the emission profile of **2d** upon water exposure at 100 °C was in line with the TGA under controlled humidity and with PXRD studies (Figure S17). Significantly, short-term exposure of **2d** to NH_3 at this temperature did not cause any structural changes, as verified by PXRD (Figure S18), and the emission maximum could be reversed to the original wavelength by evacuating the NH_3-exposed sample for 15 min (Figure S14). To further test

the potential damage caused by NH_3 exposure, we immersed samples of **2d** in DMSO-d_6 before and after the ammonia exposure. As shown in Figure S19, neither experiment showed evidence of ligand in solution, as might be expected upon leakage of H_2DHBDC^{2-} from damaged samples. Together, these results show that ammonia sensing in **2d** is selective over important atmospheric interferents, including H_2O and CO_2, at 100 °C. The selective detection of ammonia is reversible upon evacuation, portending potential applications in real devices.

To investigate the mechanism that gives rise to selectivity in **2**, we performed in situ IR studies under conditions mimicking those employed for the fluorescence measurements. Thus, IR spectroscopy of **2d** under NH_3 exposure at 100 °C revealed new peaks that could be associated with unbound NH_3 molecules (Figure S20) but did not reveal the presence of Mg−N stretches (ν_{Mg-N}). As such, we considered alternative sensing mechanisms and addressed the possibility of NH_3 interacting directly with the ligand, especially with the free −OH groups. To examine whether the free ligand, H_4DHBDC, could itself function as a reversible ammonia sensor, for instance, a sample was exposed to NH_3 vapors at room temperature and at 100 °C. In contrast to **2d**, where an emission shift and a turn-on response were recorded, exposure of H_4DHBDC to NH_3 caused the formation of a new, non-emissive, crystalline material (Figure 5). We were able to identify this new material as the ammonium salt (NH_4)-(H_3DHBDC) by independently synthesizing it from H_4DHBDC and aqueous ammonium hydroxide and confirming its structure by X-ray crystallography (Table S3, Figure S21).

Because treatment of H_4DHBDC with NH_3 did not cause deprotonation of the phenol groups, we do not expect that a chemical interaction between NH_3 and the ligand itself is responsible for the turn-on response observed in **2d**. Furthermore, the carboxylate groups in **2d** are engaged in bonding to Mg^{2+} and are obviously not available for further deprotonation. Therefore, we propose that the selective response is indeed due to direct binding of NH_3 to the Mg^{2+} sites, and that the changes in the electronic structure at the metal site inductively affect the HOMO and LUMO energies of the H_2DHBDC^{2-} linker. Although a charge-transfer mechanism whereby NH_3 molecules affect the orbital energies of H_2DHBDC^{2-} directly (i.e., through space) cannot be ruled out, such a mechanism should also be activated upon exposure to water vapor. Furthermore, the absence of ν_{Mg-N} bands need not indicate the lack of NH_3 binding at Mg^{2+} sites. Instead, it may be due to the low concentration of Mg−NH_3 pairs or the concealment of ν_{Mg-N} by stronger framework bands in the low-frequency/far-IR region. As with **1**, this hypothesis is also
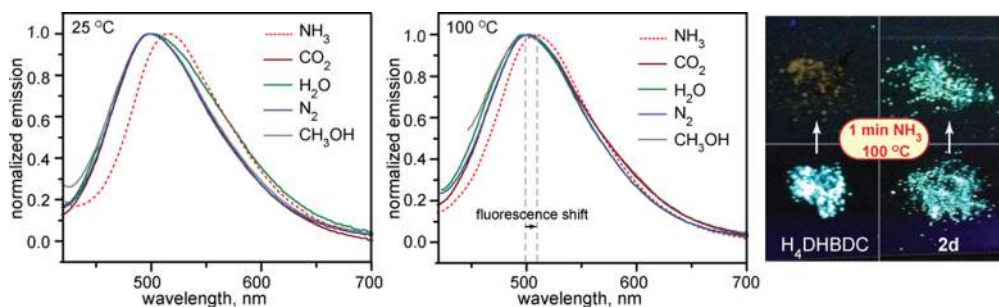

Figure 5. In situ emission spectra of **2d** when exposed to various analytes at room temperature and 100 °C. The optical micrographs display the changes in the luminescence response upon exposure of H_4DHBDC and **2d** to ammonia for 1 min at 100 °C.

supported by DFT calculations of the interaction of NH_3 with a truncated model of **2d**, which showed that ammonia binding is more favorable than water binding by 19 kJ/mol (Table S1). Although our calculations suggest that methanol and ammonia should have similar binding energies, we partially ascribe the selectivity for the former to the small pores of **2d**[25] and the larger kinetic diameter, k_D, of CH_3OH (k_D = 3.8−4.1 Å)[27] compared to NH_3 (k_D = 2.6 Å)[28] and water (k_D = 2.65 Å).[29] A combination of molecular sieving and chemical selectivity is therefore responsible for the unique NH_3 sensing properties of **2d**.

The foregoing results demonstrate that MOFs remain emissive up to high temperatures, a property that is likely general for many fluorescent MOFs because of their rigidity. This stands on its own as an interesting effect that is seldom replicated in organic molecular crystals or flexible polymers and may serve to study the photophysics of chromophores under unusual conditions. Here, we use this effect to show that temperature can be employed as an easily tunable parameter to increase the chemical selectivity in molecular sensing applications. In doing so, we demonstrate a new, reversible, and selective sensor for ammonia, an important environmental pollutant.

■ ASSOCIATED CONTENT

Ⓢ Supporting Information

X-ray structure refinement table; NMR, IR, and fluorescence spectra; DFT-calculated binding energies; TGA plot; and PXRD patterns. This material is available free of charge via the Internet at http://pubs.acs.org.

■ AUTHOR INFORMATION

Corresponding Author

mdinca@mit.edu

Notes

The authors declare no competing financial interest.

■ ACKNOWLEDGMENTS

■ REFERENCES

(1) Yaghi, O. M.; Li, H.; Groy, T. L. *J. Am. Chem. Soc.* **1996**, *118*, 9096−9101.

(2) Shekhah, O.; Liu, J.; Fischer, R. A.; Wöll, C. *Chem. Soc. Rev.* **2011**, *40*, 1081−1106.

(3) Li, M.; Dincă, M. *J. Am. Chem. Soc.* **2011**, *133*, 12926−12929.

(4) Allendorf, M. D.; Bauer, C. A.; Bhakta, R. K.; Houk, R. J. T. *Chem. Soc. Rev.* **2009**, *38*, 1330−1352.

(5) Cui, Y.; Yue, Y.; Qian, G.; Chen, B. *Chem. Rev.* **2012**, *112*, 1126−1162.

(6) Kreno, L. E.; Leong, K.; Farha, O. K.; Allendorf, M.; Van Duyne, R. P.; Hupp, J. T. *Chem. Rev.* **2012**, *112*, 1105−1125.

(7) Lin, J.; Hu, Q.-S.; Xu, M.-H.; Pu, L. *J. Am. Chem. Soc.* **2002**, *124*, 2088−2089.

(8) Kuppler, R. J.; Timmons, D. J.; Fang, Q.-R.; Li, J.-R.; Makal, T. A.; Young, M. D.; Yuan, D.; Zhao, D.; Zhuang, W.; Zhou, H.-C. *Coord. Chem. Rev.* **2009**, *253*, 3042−3066.

(9) Cui, Y.; Xu, H.; Yue, Y.; Guo, Z.; Yu, J.; Chen, Z.; Gao, J.; Yang, Y.; Qian, G.; Chen, B. *J. Am. Chem. Soc.* **2012**, *134*, 3979−3982.

(10) Rocha, J.; Carlos, L. D.; Paz, F. A.; Ananias, D. *Chem. Soc. Rev.* **2011**, *40*, 926−940.

(11) Chen, B. L.; Xiang, S. C.; Qian, G. D. *Acc. Chem. Res.* **2010**, *43*, 1115−1124.

(12) Pramanik, S.; Zheng, C.; Zhang, X.; Emge, T. J.; Li, J. *J. Am. Chem. Soc.* **2011**, *133*, 4153−4155.

(13) Xie, Z.; Ma, L.; DeKrafft, K. E.; Jin, A.; Lin, W. *J. Am. Chem. Soc.* **2010**, *132*, 922−923.

(14) Barrett, S. M.; Wang, C.; Lin, W. *J. Mater. Chem.* **2012**, *22*, 10329−10334.

(15) Li, Y.; Zhang, S.; Song, D. *Angew. Chem., Int. Ed.* **2013**, *52*, 710−713.

(16) Takashima, Y.; Martínez, V. M.; Furukawa, S.; Kondo, M.; Shimomura, S.; Uehara, H.; Nakahama, M.; Sugimoto, K.; Kitagawa, S. *Nature Commun.* **2011**, *2*, 168.

(17) Uchiyama, S.; Matsumura, Y.; de Silva, A. P.; Iwai, K. *Anal. Chem.* **2003**, *75*, 5926−5935.

(18) Pietsch, C.; Vollrath, A.; Hoogenboom, R.; Schubert, U. S. *Sensors* **2010**, *10*, 7979−7990.

(19) Li, L.; Gao, P.; Baumgarten, M.; Müllen, K.; Lu, N.; Fuchs, H.; Chi, L. *Adv. Mater.* **2013**, *25*, 3419−3425.

(20) Shustova, N. B.; McCarthy, B. D.; Dincă, M. *J. Am. Chem. Soc.* **2011**, *133*, 20126−20129.

(21) Shustova, N. B.; Cozzolino, A. F.; Dincă, M. *J. Am. Chem. Soc.* **2012**, *134*, 19596−19599.

(22) Shustova, N. B.; Ong, T.-C.; Cozzolino, A. F.; Michaelis, V. K.; Griffin, R. G.; Dincă, M. *J. Am. Chem. Soc.* **2012**, *134*, 15061−15070.

(23) We note that desolvated **1** can be heated up to 350 °C in air without losing its crystallinity or undergoing a phase change (Figure 2).

(24) Banerjee, M.; Emond, S. J.; Lindeman, S. V; Rathore, R. *J. Org. Chem.* **2007**, *72*, 8054−8061.

(25) Jayaramulu, K.; Kanoo, P.; George, S. J.; Maji, T. K. *Chem. Commun.* **2010**, *46*, 7906−7908.

(26) Wade, C. R.; Corrales-Sanchez, T.; Narayan, T. C.; Dincă, M. *Energy Environ. Sci.* **2013**, *6*, 2172−2177.

(27) Ten Elshof, J. E.; Abadal, C. R.; Sekulić, J.; Chowdhury, S. R.; Blank, D. H. A. *Microporous Mesoporous Mater.* **2003**, *65*, 197−208.

(28) Reineke, T. M.; Eddaoudi, M.; Fehr, M.; Kelley, D.; Yaghi, O. M. *J. Am. Chem. Soc.* **1999**, *121*, 1651−1657.

(29) D'Alessandro, D. M.; Smit, B.; Long, J. R. *Angew. Chem., Int. Ed.* **2010**, *49*, 6058−6082.